monotonic decrease in fractionation factors approaching the value for aqueous L_3O^+ (0.69). The data for the $L_9O_4^+$ cluster (Table III) are of comparable quality to those for the $L_7O_3^+$ and $L_5O_2^+$ clusters (Tables I and II, respectively) in terms of reproducibility. The sudden increase in fractionation factor observed for the tetramer may result from the accessibility of alternative low-energy structures (e.g., **6**) such that bridging and terminal positions are

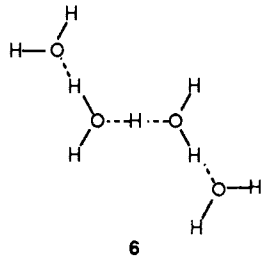

6

less well-defined than in **1-3**. Alternatively, the tetramer cluster may have a higher effective internal temperature, as a result either of incomplete thermal equilibration in the flow tube or of collisional activation in the lenses of the sampling system.

Conclusions

The product distributions resulting from CID of partially deuterated water cluster ions reflect a preference for fractionation of deuterium to the neutral CID product. The fractionation appears to be independent of collision energy within experimental error and is therefore identified as resulting from an equilibrium isotope effect that acts to alter the equilibrium distribution of cluster isotopomers. This fractionation effect appears to be the same effect observed in gas-phase bimolecular isotope-exchange reactions and in condensed-phase isotope fractionation. The values for the fractionation factors of gaseous L_3O^+ and $L_5O_2^+$ resulting from the present data are only slightly lower than those observed for the equilibrium exchange reactions.[26,27] This difference may be a consequence of different internal energies for the cluster ions in the present study compared to the corresponding intermediates in the equilibrium reactions and/or a difference in the effective temperature at which the fractionation occurs. Fractionation factors for stepwise deuteration in each of the $(L_2O)_nL^+$ (n = 2-4) species display dependence on deuterium content, increasing toward unity as the deuterium content increases. We intend to continue our study of isotope fractionation in cluster ion CID with investigations of the NH_4^+/ND_3 system, in which D is predicted to preferentially migrate to the *ionic* products of the bimolecular exchange reaction[32,57] and therefore should also fractionate to the ionic products of activated unimolecular decomposition. Other systems of potential interest include the anionic clusters $OL^-(L_2O)_n$ and mixed species such as $CH_3OL_2^+(L_2O)$.

Acknowledgment. Support of this work by the National Science Foundation (Grant CHE-8502515) is gratefully acknowledged. R.R.S. thanks the Alfred P. Sloan Foundation for a fellowship and S.T.G. acknowledges the David Ross Foundation for fellowship support.

A Transient Infrared Spectroscopy Study of Coordinatively Unsaturated Osmium Carbonyl Compounds

Paula L. Bogdan and Eric Weitz*

Contribution from the Department of Chemistry, Northwestern University, Evanston, Illinois 60208. *Received June 5, 1989*

Abstract: Transient infrared spectroscopy is used to study the coordinatively unsaturated osmium carbonyl fragments generated by 248-nm photolysis of gas-phase $Os(CO)_5$. The nascent photoproducts, predominantly $Os(CO)_3$ with some $Os(CO)_4$, are highly reactive toward combination with both CO and $Os(CO)_5$. The bimolecular rate constants for reaction of $Os(CO)_3$ and $Os(CO)_4$ with CO are 7.6 ± 0.9 and $5.5 \pm 0.6 \times 10^{-11}$ cm^3 molecule^{-1} s^{-1}, respectively. Infrared absorptions for a new unsaturated osmium species, $Os_2(CO)_8$, formed by reaction of $Os(CO)_3$ with $Os(CO)_5$, are assigned. The rate constant for this reaction is $2.7 \pm 0.9 \times 10^{-10}$ cm^3 molecule^{-1} s^{-1}, on the order of gas kinetic. The reactivities of the unsaturated osmium species are similar to those of the analogous ruthenium compounds and contrast with the reactivity of $Fe(CO)_4$. The trends observed in the photochemistry of group 8 metal carbonyl complexes and the role of spin selection rules in the reactivity of these coordinatively unsaturated fragments are discussed. Continuing depletion of the $Os(CO)_5$ parent after photolysis indicates that polynuclear osmium carbonyl clusters are formed.

Studies of unsaturated metal carbonyl compounds continue to be of fundamental interest because of their central role in stoichiometric and catalytic reaction processes.[1,2] An understanding of the structure and reactivity patterns of these key intermediates can be beneficial in the design of new catalysts, solid-state materials, and thin-film coatings.

Transient infrared spectroscopy is a powerful tool in the study of unsaturated metal carbonyl complexes.[3] The technique can provide both kinetic and structural information for transient species. Both gas-phase and solution-phase measurements have been performed. Advantages of gas phase studies are that multiple open coordination sites can be generated by photolysis and the species generated are free from solvation effects.

To date, a variety of metal carbonyl compounds has been investigated with transient infrared spectroscopy.[4-6] Some of the most intriguing results have been reported for photofragments of iron pentacarbonyl.[7] The rate constants for the reaction of $Fe(CO)_4$ with CO and with $Fe(CO)_5$ are approximately 10^3

(1) Ugo, R., Ed. *Aspects of Homogeneous Catalysis*; D. Reidel: Dordrecht, The Netherlands, 1984; Vol. 5.
(2) Twigg, M. V., Ed. *Mechanisms of Inorganic and Organometallic Reactions*; Plenum Press: New York, 1986; Vol. 4, Part 3.
(3) Weitz, E.; Poliakoff, M. *Adv. Organomet. Chem.* **1986**, *25*, 277.
(4) Weitz, E. *J. Phys. Chem.* **1987**, *91*, 3945.
(5) Schaffner, K.; Grevels, F.-W. *J. Mol. Struct.* **1988**, *173*, 51.
(6) Ishikawa, Y.; Hackett, P. A.; Rayner, D. M. *J. Mol. Struct.* **1988**, *174*, 113.
(7) Poliakoff, M.; Weitz, E. *Acc. Chem. Res.* **1987**, *20*, 408.

0002-7863/90/1512-639$02.50/0

smaller than the analogous rate constants for any other monometallic carbonyl complex with vacant coordination sites.[4-6] Spin selection rules are thought to be responsible for the relative magnitude of the rate constants in the $Fe(CO)_5$ system. The $Fe(CO)_4$ fragment possesses a triplet electronic ground state,[8] so that its reaction with singlet CO to generate singlet $Fe(CO)_5$ or with $Fe(CO)_5$ to generate $Fe_2(CO)_9$ is not spin allowed. We recently reported studies on the second member of the group 8 triad, $Ru(CO)_5$, and found very fast reaction rates for all the ruthenium photofragments.[9] It is of interest then to complete the time-resolved studies on this triad and determine whether the behavior of unsaturated osmium carbonyl compounds is more similar to iron or ruthenium. We can then compare the results for all three metals and see what implications this has for the chemistry of the group 8 carbonyl compounds.

Experimental Section

The apparatus used in this study has been previously described.[10-13] Since it is both expensive and inconvenient to prepare the amount of $Os(CO)_5$ that would be needed for a flow cell, an experimental procedure involving static cell fills, as was employed in the study of $Ru(CO)_5$, was used for these experimental measurements.[9] After each set of measurements, the cell is evacuated and then recharged. In the experiments with $Ru(CO)_5$, CO was added to the cell fills to retard decomposition. Though $Os(CO)_5$ is both light and heat sensitive, it has greater stability than $Ru(CO)_5$, and addition of CO to retard adventitious decomposition is not necessary. However, it is necessary to clean osmium cluster deposits from the cell windows periodically.

The output of a UV excimer laser (Questek) operating at 248 nm (KrF) is used to photolyze $Os(CO)_5$. Formation of unsaturated osmium carbonyl photoproducts is detected by their attenuation of infrared radiation from a home-built liquid-nitrogen-cooled CO laser. Infrared beam intensity is measured with a fast (τ_{rise} = 35 ns) InSb detector. The detector output (transient waveform) is amplified (Perry X100), digitized, signal averaged (Lecroy 9400), and sent to a computer for storage and manipulation. Time-resolved infrared spectra of the transients are constructed from the waveforms acquired at probe frequencies within the carbonyl stretch region by joining together the amplitude of various waveforms at common delay times.

Typical pressures of $Os(CO)_5$ in the cell were on the order of 40–200 mTorr. The infrared signals from each cell fill were normalized by comparing the attenuation of the excimer laser beam as measured by a photodiode. The difference in the magnitudes of the photodiode signals acquired during photolysis and after the cell is evacuated is proportional to the amount of $Os(CO)_5$ photolyzed. Excimer laser energies at the cell were approximately 2–3 mJ/cm^2. All experiments were performed at ambient temperature, 21 ± 1 °C.

Kinetic information is obtained by probing the relevant regions of the time-resolved infrared spectrum while varying the concentration of added CO. Resulting waveforms are analyzed as multiple exponentials by a Provencher routine.[14]

Measurements of UV-vis and IR spectra of $Os(CO)_5$ vapor were made with Perkin-Elmer 331 and Matheson Polaris spectrophotometers, respectively.

Neat $Os(CO)_5$[15,16] was generously provided by Prof. J. Takats and G.-Y. Kiel of the University of Alberta. The gases used for the experiments (CO and Ar) were obtained from Matheson and had stated purities of 99.995%.

Results

Assignments. Osmium pentacarbonyl was first reported in 1943[17] and was assigned a trigonal-bipyramidal structure on the basis of its infrared spectrum.[15] A recent gas-phase electron-diffraction study has confirmed this structural assignment.[18] Figure 1 shows the CO stretching bands in the infrared region for $Os(CO)_5$ in the gas phase, with absorptions assigned to the e mode at 2008 and the a_2 mode at 2046 cm^{-1}. The small peak at 1960 cm^{-1} is due to the presence of natural abundance ^{13}CO in the sample. The absorption coefficient for the low-frequency band of $Os(CO)_5$ was calculated as 0.15 ± 0.04 cm^{-1} Torr^{-1}. The value compares well with 0.12 cm^{-1} Torr^{-1}, which was calculated with data from a previously published spectrum of $Os(CO)_5$.[19]

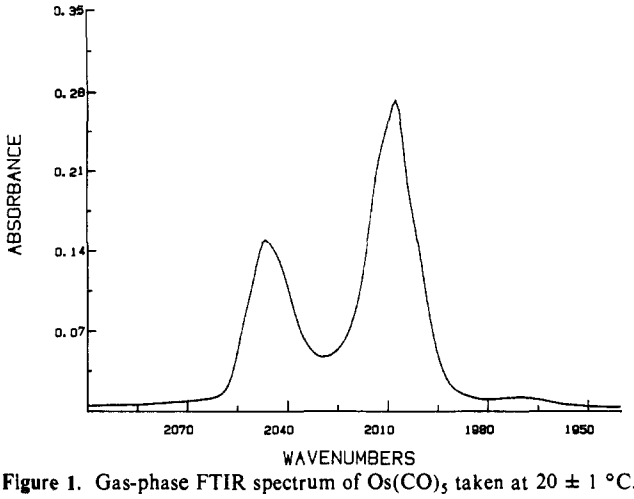

Figure 1. Gas-phase FTIR spectrum of $Os(CO)_5$ taken at 20 ± 1 °C.

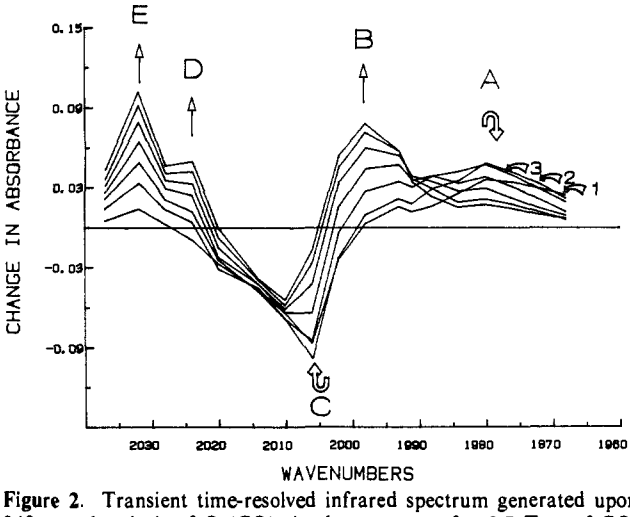

Figure 2. Transient time-resolved infrared spectrum generated upon 248-nm photolysis of $Os(CO)_5$ in the presence of ~0.7 Torr of CO. Spectral traces are separated by 0.1-μs intervals and arrows indicate the direction of the peaks. The lowest frequency peak rises for the first three traces and then begins to decay. The labeled peaks are assigned as follows: A, $Os(CO)_3$; B, $Os(CO)_4$; C, $Os(CO)_5$; D, $Os_2(CO)_8$; E, $Os(CO)_4$.

Time-resolved infrared measurements were obtained with use of static cell fills of $Os(CO)_5$ vapor. Though not as robust as $Fe(CO)_5$, $Os(CO)_5$ is more stable than $Ru(CO)_5$ and does not decompose as readily in the absence of added CO. Hence one can obtain transient IR signals for photoproducts of $Os(CO)_5$ without added CO. However, there are some unique difficulties in studying $Os(CO)_5$ versus $Ru(CO)_5$. These result from the relatively small UV cross section for the osmium species. It was not possible to obtain signals with 351-nm (XeF) irradiation with less than 0.5 Torr of $Os(CO)_5$ in a 16 cm path length cell. Pressures of at least 40 mTorr are required to obtain good quality signals with 248-nm (KrF) photolysis. At pressures of $Os(CO)_5$ greater than ~0.2 Torr, it becomes difficult to measure transients

(8) Barton, T. J.; Grinter, R.; Thomson, A. J.; Davies, B.; Poliakoff, M. *J. Chem. Soc., Chem. Commun.* **1977**, 841.
(9) Bogdan, P. L.; Weitz, E. *J. Am. Chem. Soc.*, in press.
(10) Ouderkirk, A. J.; Weitz, E. *J. Chem. Phys.* **1983**, *79*, 1089.
(11) Ouderkirk, A. J.; Wermer, P.; Schultz, N. L.; Weitz, E. *J. Am. Chem. Soc.* **1983**, *105*, 3354.
(12) Ouderkirk, A. J.; Seder, T. A.; Weitz, E. *SPIE* **1984**, *458*, 148.
(13) Seder, T. A.; Church, S. P.; Weitz, E. *J. Am. Chem. Soc.* **1985**, *107*, 1432.
(14) Provencher, S. W. *Biophys. J.* **1976**, *16*, 27; *J. Chem. Phys.* **1976**, *64*, 2772.
(15) Calderazzo, F.; L'Eplattenier, F. *Inorg. Chem.* **1967**, *6*, 1220.
(16) Rushman, R.; van Buuren, G. N.; Shiralian, M.; Pomeroy, R. K. *Organometallics* **1983**, *2*, 693.
(17) Hieber, W.; Stallman, H. *Z. Elektrochem.* **1943**, *49*, 288.
(18) Huang, J.; Hedberg, K.; Pomeroy, R. K. *Organometallics* **1988**, *7*, 2049.
(19) Bristow, N. J.; Moore, B. D.; Poliakoff, M.; Ryott, G. J.; Turner, J. J. *J. Organomet. Chem.* **1984**, *260*, 181.

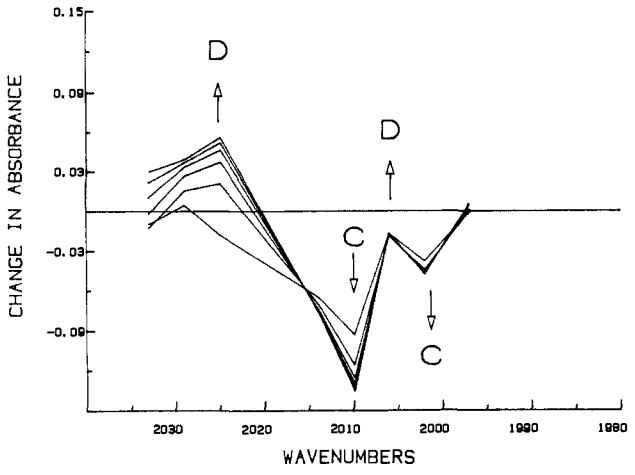

Figure 3. Transient time-resolved infrared spectrum generated upon 248-nm photolysis of $Os(CO)_5$ without added CO. Spectral traces are separated by 0.2-μs intervals and arrows indicate the direction of peaks. Labels are as in Figure 2.

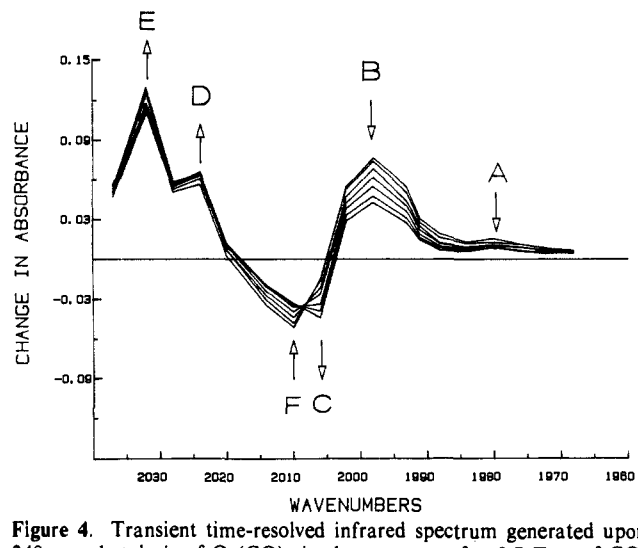

Figure 4. Transient time-resolved infrared spectrum generated upon 248-nm photolysis of $Os(CO)_5$ in the presence of ~0.7 Torr of CO, showing the time period beginning 0.8 μs after the UV laser pulse. The peak labeled F is assigned to $Os_2(CO)_9$. Other labels are as in Figure 2. Traces are separated by 1-μs intervals.

at the positions of the $Os(CO)_5$ parent IR absorptions because the cell becomes optically dense. There is a significant amount of parent depletion between UV laser slots due to formation of polynuclear osmium carbonyl species; this will be discussed in more detail. For this reason, in the absence of added CO, only one or two laser pulses were used to obtain kinetic data for reactions that are dependent on the pressure of $Os(CO)_5$. The presence of CO increases regeneration of $Os(CO)_5$ versus formation of polynuclear species. Under these conditions, the change in $Os(CO)_5$ pressure after each UV laser shot was not as dramatic and the transients resulting from ten laser pulses could be averaged without a significant change in the rate or shape of the transients. Thus, it was convenient to acquire the transient signals in the presence of added CO, except when reactions involving CO competed with the reaction of interest.

The time-resolved infrared spectrum of $Os(CO)_5$ in the presence of 0.7 Torr of CO is shown in Figure 2. The parent absorption at 2006 cm^{-1} shows initial depletion upon photolysis and is regenerated by reaction of the photoproducts with CO. There are at least four other species present that can be identified on the basis of their absorption bands and time scale and kinetics of formation. In the absence of CO, the 1980-cm^{-1} absorption (A) retains its large, detector-limited rise, while the 2000-cm^{-1} absorption (B) shows a very small, detector-limited, rise. In addition, the rise of B shows a significant CO pressure dependence, while the rise of A does not. This indicates that the primary reaction photoproduct at this wavelength is species A and that most of the B present in the Figure 2 spectrum arises from reaction of A with CO. The A absorption at ~1980 cm^{-1} is assigned to $Os(CO)_3$, and the B band with apparent maximum at ~2000 cm^{-1} is assigned to $Os(CO)_4$. Confirming this assignment is the fact that internal excitation is apparent in $Os(CO)_4$ (band B), as manifested by an initial narrowing and rapid shifting of the band B to higher frequency as the internally excited $Os(CO)_4$ relaxes. Species $Os(CO)_3$ (band A) is formed with much less internal excitation as is expected for a more highly coordinatively unsaturated species.[3] Figure 3 shows a portion of the time-resolved spectrum recorded in the absence of added CO pressure. There is a shift of the $Os(CO)_5$ band maximum to higher wavenumbers in this spectrum relative to Figure 2. The $Os(CO)_4$ band (largely absent in Figure 3) substantially overlaps with parent in Figure 2, and thus the true absorption maximum for $Os(CO)_4$ is likely very close to that of the parent. There is a strong depletion of the parent band (2010 cm^{-1}, C) after initial photolysis that has the same temporal behavior as the decay of the $Os(CO)_3$ transient at 1980 cm^{-1}. The product of this reaction is assigned as $Os_2(CO)_8$; though not previously reported for osmium, the $M_2(CO)_8$ complex has been characterized in a matrix for M = Fe.[20,21] On the basis of Figure 3, we have assigned two absorptions (D) for $Os_2(CO)_8$ at ca. 2024 cm^{-1}, and one that overlaps $Os(CO)_5$ at ca. 2005 cm^{-1}. The absorption labeled E in Figure 2 increases in intensity with added CO. Since adding CO increases the amount of $Os(CO)_4$ present, E is assigned as another absorption band of $Os(CO)_4$. Consistent with this assignment, absorption bands B + E grow in the same rate. However, the E band does not decay with the same temporal profile as B (Figure 4) because of underlying absorptions believed due to polynuclear osmium carbonyl compounds. The presence of a high-frequency absorption for $Os(CO)_4$ is consistent with the position of CO stretches in the spectrum of $Os(CO)_4$(benzene) obtained with time-resolved spectroscopy in solution.[22]

The time-resolved spectrum (with 0.7 Torr of added CO) beginning 0.8 μs after the UV photolysis is shown in Figure 4. By 0.8 μs, most of the $Os(CO)_3$ has reacted with CO and the predominant species are $Os(CO)_4$ and $Os(CO)_5$. The presence of an isosbestic point at ~2010 cm^{-1} indicates that $Os(CO)_5$ is being consumed to give primarily one product in this time period. Its most likely reaction partner is $Os(CO)_4$ (to form $Os_2(CO)_9$), though reaction with $Os_2(CO)_8$ (formed by reaction of $Os(CO)_3$ and $Os(CO)_5$) is also possible. However, this latter reaction is unlikely; the amount of $Os_2(CO)_8$ formed from typically 50 mTorr of $Os(CO)_5$ in the presence of 0.7 Torr of added CO is small because under these conditions $Os(CO)_3$ reacts quickly with CO to form $Os(CO)_4$. Thus, absorption F is most likely due to the dinuclear osmium carbonyl complex, $Os_2(CO)_9$. Previous reports of the IR spectral characterization of $Os_2(CO)_9$ exist, listing absorptions at 2028 s, 2038 vs, 2024 m, 2013 s, 2000 w, 1778 m cm^{-1} (heptane).[23] Absorption F is compatible with the reported 2013-cm^{-1} band of $Os_2(CO)_9$. However, because of the number of species absorbing in the transient spectrum in the region above 2000 cm^{-1}, it is not possible to resolve all of the terminal bands of $Os_2(CO)_9$ observed in solution. Thus, in order to confirm the presence of $Os_2(CO)_9$, we examined the lower wavenumber region of the spectrum to locate the expected bridging CO band of $Os_2(CO)_9$. This band was found at 1794 cm^{-1}. This bridging CO band becomes more intense and grows in more quickly in the presence of added CO. These observations are compatible with a species formed from reaction of $Os(CO)_4$ and parent $Os(CO)_5$,

(20) Poliakoff, M.; Turner, J. J. *J. Chem. Soc. A*, **1971**, 2403.

(21) We just learned that $Os_2(CO)_8$ has been characterized in matrix and solution studies: (a) Haynes, A.; Poliakoff, M.; Turner, J. J.; Bender, B. R.; Norton, J. R. Submitted for publication. (b) Grevels, F.-W. Personal communication from J. Takats.

(22) Church, S. P.; Grevels, F.-W.; Kiel, G.-Y.; Kiel, W. A.; Takats, J.; Schaffner, K. *Angew. Chem., Int. Ed. Engl.* **1986**, *25*, 991.

(23) Moss, J. R.; Graham, W. A. G. *J. Chem. Soc., Dalton Trans.* **1977**, 95.

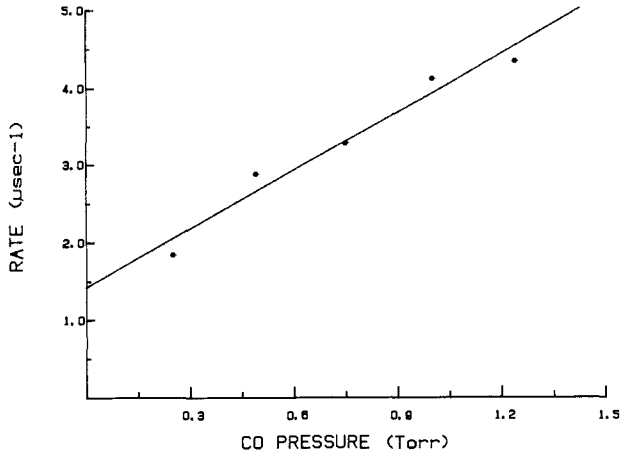

Figure 5. Plot of the pseudo-first-order rate constant for the reaction of $Os(CO)_3$ with CO. The rate of disappearance of $Os(CO)_3$ at 1980 cm^{-1} is plotted against the pressure of added CO. The slope of the line gives a bimolecular rate constant of $7.6 \pm 0.9 \times 10^{-11}$ cm^3 $molecule^{-1}$ s^{-1} for the $Os(CO)_3 + CO \rightarrow Os(CO)_4$ reaction.

rather than $Os(CO)_3$ and parent. Thus the absorption can be unambiguously assigned to $Os_2(CO)_9$ rather than $Os_2(CO)_8$. If this bridging band belonged to $Os_2(CO)_8$, the signal amplitude would *decrease* in the presence of CO, since CO will compete with $Os(CO)_5$ as a reactant for $Os(CO)_3$ (eq iii vs v in Scheme I). This absorption at 1794 cm^{-1} and absorption F at approximately 2014 cm^{-1} are then assigned as $Os_2(CO)_9$ absorptions. This assignment is consistent with the recent report that matrix-isolated $Os_2(CO)_8$ does *not* have a bridging CO.[21]

The proposed scheme for reactions on a short time scale following 248-nm photolysis of $Os(CO)_5$ is shown in Scheme I.

Scheme I

$$Os(CO)_5 \xrightarrow{h\nu} Os(CO)_3 + 2\ CO \quad \text{(i)}$$

$$Os(CO)_5 \xrightarrow{h\nu} Os(CO)_4 + CO \quad \text{(ii)}$$

$$Os(CO)_3 + CO \rightarrow Os(CO)_4 \quad \text{(iii)}$$

$$Os(CO)_4 + CO \rightarrow Os(CO)_5 \quad \text{(iv)}$$

$$Os(CO)_3 + Os(CO)_5 \rightarrow Os_2(CO)_8 \quad \text{(v)}$$

$$Os(CO)_4 + Os(CO)_5 \rightarrow Os_2(CO)_9 \quad \text{(vi)}$$

On a longer time scale, the absorption due to parent $Os(CO)_5$ continues to decay. Transient absorptions assigned to $Os_2(CO)_8$ also decay with the same rate. The identity of the product of the reaction of $Os(CO)_5$ with $Os_2(CO)_8$ is not known for certain, but it may be $Os_3(CO)_{12}$. A further depletion of parent is observed on a time scale well beyond that for complete disappearance of $Os_2(CO)_8$. Ultimately, a pale yellow film is observed on the bottom of the gas cell. In the case of $Ru(CO)_5$ photolysis, a uniform film of $Ru_3(CO)_{12}$ eventually covers all parts of the gas cell. For osmium, nucleation to form large non-volatile particles appears to take place in the gas phase, as opposed to on the walls of the cell. The amount of parent $Os(CO)_5$ depleted per laser shot is approximately three times the amount of $Os(CO)_5$ actually photolyzed, but formation of clusters of higher nuclearity than $Os_3(CO)_{12}$ cannot be ruled out. A large number of binary metal carbonyl compounds of osmium are in fact known.[24] The only product observed by solution infrared spectroscopy upon extraction of the cell residue is $Os_3(CO)_{12}$; however, it would not be surprising for the larger clusters to degrade to the stable triosmium cluster upon standing for extended periods of time.[24]

Kinetics. Reaction rates for recombination of the photofragments $Os(CO)_3$ and $Os(CO)_4$ with CO were determined from the slope of the line obtained from plotting the decay rate of the appropriate transient signal versus CO pressure (Figure 5). Kinetic measurements were performed by monitoring the disappearance of $Os(CO)_3$ and $Os(CO)_4$ at 1990 and 1998 cm^{-1}, respectively. To minimize competition from polynuclear osmium reactions, the smallest convenient amount of $Os(CO)_5$ was used (~40 mTorr). The bimolecular rate constants for $Os(CO)_3 + CO$ (eq 1) and $Os(CO)_4 + CO$ (eq 2) are 7.6 ± 0.9 and $5.5 \pm 0.6 \times 10^{-11}$ cm^3 $molecule^{-1}$ s^{-1}. These values are very similar to those obtained for the CO addition reactions of the analogous ruthenium carbonyl species (7.6 and 2.8×10^{-11} cm^3 $molecule^{-1}$ s^{-1}).[9] These rate constants are approximately one-tenth of the gas kinetic value.

Table I. Bimolecular Reaction Rate Constants for Group 8 Unsaturated Metal Carbonyl Species with CO

	rate constant, $\times 10^{-11}$ cm^3 $molecule^{-1}$ s^{-1}	ref
$Fe(CO)_4$	0.006	30
$Fe(CO)_3$	2	30
$Fe(CO)_2$	3	30
$Ru(CO)_4$	3	9
$Ru(CO)_3$	8	9
$Os(CO)_4$	5	*a*
$Os(CO)_3$	8	*a*

[a] This work.

Table II. Bimolecular Rate Constants for Reaction of Group 8 Unsaturated Metal Carbonyl Species with Parent $M(CO)_5$

	product	rate constant, $\times 10^{-10}$ cm^3 $molecule^{-1}$ s^{-1}	ref
$Fe(CO)_3$	$Fe_2(CO)_8$ (bridged)	3	25
$Fe(CO)_4$	$Fe_2(CO)_9$	0.005	25
$Fe_2(CO)_8$	$Fe_3(CO)_{12}$	~1	25
$Ru(CO)_4$	$Ru_2(CO)_9$	~10	9
$Os(CO)_3$	$Os_2(CO)_8$	3	*a*
$Os(CO)_4$	$Os_2(CO)_9$	~1	*a*
$Os_2(CO)_8$	$Os_3(CO)_{12}$?	~1	*a*

[a] This work.

$$Os(CO)_3 + CO \xrightarrow{k_1} Os(CO)_4 \quad (1)$$

$$Os(CO)_4 + CO \xrightarrow{k_2} Os(CO)_5 \quad (2)$$

In addition, the bimolecular rate constant for reaction of $Os(CO)_3$ with $Os(CO)_5$ has been determined by using measurements in which the pressure of $Os(CO)_5$ was varied in the absence of CO. For this purpose, the decay of the $Os(CO)_3$ transient at 1980 cm^{-1} was monitored over a 10-μs time interval. The rate constant for reaction 3 is $2.7 \pm 0.9 \times 10^{-10}$ cm^3 $molecule^{-1}$ s^{-1}. This is comparable to the value obtained for the reaction of $Fe(CO)_3$ with $Fe(CO)_5$ to form the bridged form of $Fe_2(CO)_8$ (Table II).[25] The

$$Os(CO)_3 + Os(CO)_5 \xrightarrow{k_3} Os_2(CO)_8 \quad (3)$$

amount of $Os(CO)_5$ in the cell can change drastically over the course of several UV shots because of continued scavenging of the parent by photoproducts to form cluster compounds. This necessitated the use of an average of only one or two transients for each measurement at a given $Os(CO)_5$ pressure. The resultant decrease in the quality of the signals and the resultant fit is the source of the larger error brackets for this measurement.

There is further depletion of the parent $Os(CO)_5$ on a time scale that parallels a decay in the absorptions attributed to $Os_2(CO)_8$ (Figure 6, 3). The correspondence between the temporal behavior of the absorptions due to $Os(CO)_5$ and $Os_2(CO)_8$ indicates that the reaction shown in eq 4 is occurring. This reaction was monitored by observing the parent absorption at 2010–2002 cm^{-1}. For the same reasons alluded to previously for k_3, it is difficult

(24) Johnston, V. J.; Einstein, F. W. B.; Pomeroy, R. K. *J. Am. Chem. Soc.* **1987**, *109*, 8111.

(25) Ryther, R.; Weitz, E. Manuscript in preparation.

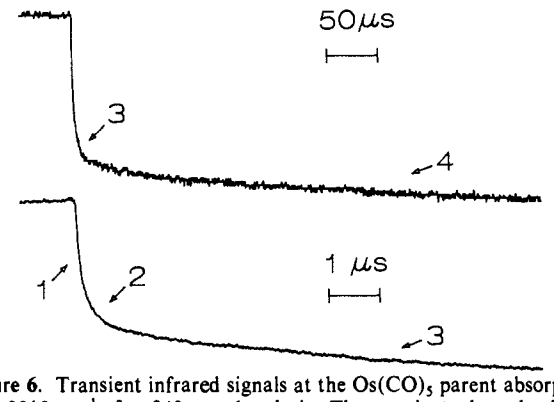

Figure 6. Transient infrared signals at the $Os(CO)_5$ parent absorption at ~2010 cm^{-1} after 248-nm photolysis. The transients show the decay of the $Os(CO)_5$ absorption on 500-μs (top) and 10-μs (bottom) time scales. Region 1 is the initial detector-limited photolysis of $Os(CO)_5$. Depletion 2 corresponds to reaction of $Os(CO)_5$ with $Os(CO)_3$. Further loss of $Os(CO)_5$ (3) is due to reaction of $Os(CO)_5$ with $Os_2(CO)_8$. The transient continues to decay slowly on a longer time scale, 4 (see text).

to determine k_4 accurately. However, k_4 is on the order of 10^{-11} cm^3 $molecule^{-1}$ s^{-1}. The rate constant for the corresponding reaction for $Fe(CO)_5$ has been determined and is similar.[25] The

$$Os_2(CO)_8 + Os(CO)_5 \xrightarrow{k_4} Os_x(CO)_y + nCO \qquad (4)$$

identity of the reaction product in eq 4 is unknown. On the basis of known osmium compounds and the iron chemistry, this species may be $Os_3(CO)_{12}$. However, it would then be difficult to rationalize the additional depletion of $Os(CO)_5$ that is observed (Figure 6, 4). It is unlikely that stable, saturated $Os_3(CO)_{12}$ would go on to build larger clusters under these conditions. The continued depletion of $Os(CO)_5$ beyond reaction with $Os_2(CO)_8$ may be due to a reaction with any $Os_2(CO)_9$ present or higher nuclearity clusters.

To compare the reactivities of the $M(CO)_4$ complexes for group 8 metals, it is also desirable to obtain a rate constant for reaction 5. The $M(CO)_4$ species are of particular interest due to the unusual reactivity observed for $Fe(CO)_4$. Obtaining the rate constant for reaction 5 presents a challenge in the case of osmium. It would be desirable to monitor the rate of disappearance of $Os(CO)_4$ with variation of $Os(CO)_5$ concentration without CO present, but this has associated difficulties. One problem is that the $Os(CO)_4$ absorption is overlapped by both $Os(CO)_5$ and $Os_2(CO)_8$, at 2000 and 2030 cm^{-1}. Also, there is little nascent $Os(CO)_4$; most of the $Os(CO)_4$ observed results from reaction 1, so when no CO is present, the absorption from nascent $Os(CO)_4$ is small and at least partially overlapped by absorptions of other species. Addition of CO to the cell to increase the amount of $Os(CO)_4$ present will set up a competition between reactions 2 and 5, since the rate constants for both $Os(CO)_3$ and $Os(CO)_4$ are similar.

$$Os(CO)_4 + Os(CO)_5 \xrightarrow{k_5} Os_2(CO)_9 \qquad (5)$$

We were able to observe the appearance of a small signal from the bridging CO absorption of $Os_2(CO)_9$ at 1794 cm^{-1} even in the absence of CO. The signal-to-noise ratios for these transients are not as good as those obtained probing terminal CO absorptions since the extinction coefficients for bridging CO stretches are much smaller and we are unable to average more than one or two signals because of changing parent concentration. As such, it was not possible to obtain a reliable number for the rate constant, k_5, from these data. However, the peak of the $Os_2(CO)_9$ absorption grows in at about 5 μs after photolysis of 100–200 mTorr of $Os(CO)_5$ and this rapid growth indicates that (5) is indeed a facile reaction. This result is similar to the ruthenium system and in contrast to the slow formation rate observed for $Fe_2(CO)_9$.[25] The rate constant for reaction 5 in benzene solution has been estimated as twice the rate for CO addition to $Os(CO)_4$ (eq 2) and so would be of a magnitude of 10^{-10} cm^3 $molecule^{-1}$.[22] This is consistent with rate constants for formation of dinuclear metal carbonyl compounds in every case except those involving spin-disallowed processes in the iron system.

Discussion

There are interesting qualitative aspects of the photochemistry of the unsaturated group 8 metal carbonyl species. One of the differences observed in these studies versus other members of the group 8 triad involves the branching ratios for product formation following 248-nm photolysis. The complex $Fe(CO)_2$ is observed following KrF photolysis of $Fe(CO)_5$. For both ruthenium and osmium, the predominant photoproduct with 248-nm irradiation is the $M(CO)_3$ species. There is no evidence in either of the latter two cases for appreciable quantities of $M(CO)_2$. A greater average M–CO bond dissociation energy for the second- and third-row metals is consistent with this observation and with trends seen in the solution chemistry of these compounds.

A previous methane matrix study of $Os(CO)_5$ indicates that absorptions at 1972 and 1955 cm^{-1} appear immediately upon photolysis.[26] These two bands were assigned to $Os(CO)_4$, while a second set of bands that appear when the matrix is further irradiated with a Nernst glower (2005 m, 2003 s, 1992, 1962 vs, and 1959 cm^{-1}) are assigned to $Os(CO)_4$(methane). Though there is some detector-limited appearance of IR absorptions in the 1950–60-cm^{-1} region in the gas phase, the absorptions are very small relative to those in Figures 2–4 and were not studied further. Comparison of the $Os(CO)_4$ peak positions in the gas phase to the matrix assignments shows an unusually large difference in position, about 40 cm^{-1}, relative to the shift of 10–20 cm^{-1} to higher wavenumbers usually observed for gas-phase species.[4] An assignment of the initially generated matrix species as $Os(CO)_3$ gives better agreement with the gas-phase band positions, but formation of highly unsaturated $Os(CO)_3$ in the matrix would not be expected on the basis of previous work.[7]

The infrared spectroscopic characterization of $Os_2(CO)_8$ in Ar matrix studies includes bands at 2060, 2023, and 2007 cm^{-1}.[21] The two lower frequency bands are in the region accessible to our experiments and are in good agreement with our assignments. In the matrix study, $Os_2(CO)_8$ is generated by photolysis of $Os_2(CO)_9$.

The bimolecular rate constants for reaction of $M(CO)_3$ fragments with CO are very similar for all three members of this triad (Table I). The $M(CO)_4$ species for M = Ru and Os have rate constants of the order of 10^{-11} cm^3 $molecule^{-1}$ s^{-1} for their reactions with CO. This is in contrast with the reactivity of $Fe(CO)_4$, whose rate constant for this process is three orders of magnitude smaller. Rate constants for reaction with CO have also been determined for carbonyl photofragments of chromium, vanadium, and tungsten, and are all of the order of 10^{-11} cm^3 $molecule^{-1}$ s^{-1}.[27-29] Thus $Fe(CO)_4$ is unusual because its gas-phase lifetime in the presence of CO is ~10^3 greater than any other coordinatively unsaturated monometallic carbonyl species known to date.

Formation of dinuclear metal complexes in general appears to be an extremely facile process for these coordinatively unsaturated complexes. Rate constants for reactions of the parent pentacarbonyl species with $Ru(CO)_3$, $Os(CO)_3$, and $Fe(CO)_3$, where the bridged form of $Fe_2(CO)_8$ is formed, are on the order of 10^{-10} cm^3 $molecule^{-1}$ s^{-1}, which is near gas kinetic (Table II). For both ruthenium and osmium, rate constants for formation of the $M_2(CO)_9$ species are also close to gas kinetic, while the reaction that involves $Fe(CO)_4$ and produces $Fe_2(CO)_9$ has a rate constant that is 10^3 smaller than those for ruthenium and osmium. Rate constants for similar processes involving chromium,[27] vanadium,[28]

(26) Poliakoff, M.; Turner, J. J. *J. Chem. Soc., Dalton Trans.* **1974**, 2276.
(27) Seder, T. A.; Church, S. P.; Weitz, E. *J. Am. Chem. Soc.* **1986**, *108*, 4721.
(28) Ishikawa, Y.; Hackett, P. A.; Rayner, D. M. *J. Am. Chem. Soc.* **1987**, *109*, 6644.
(29) Ishikawa, Y.; Hackett, P. A.; Rayner, D. M. *J. Phys. Chem.* **1988**, *92*, 3863.

and tungsten[29] are comparable to those for ruthenium[9] and osmium.

The explanation of the stability of the $Fe(CO)_4$ unit in the presence of CO and $Fe(CO)_5$ is based upon spin conservation rules. The $Fe(CO)_4$ complex has been characterized as possessing a ground-state triplet electronic configuration so that its reactions with either singlet CO or singlet parent to produce singlet $Fe(CO)_5$ or singlet $Fe_2(CO)_9$, respectively, are formally spin-forbidden.[8] The facile CO addition reactions for $Fe(CO)_2$ and $Fe(CO)_3$ are evidence to support the notion that all the mononuclear iron photofragments are ground-state triplets.[30] However, spin selection rules may also play a role in some polynuclear forming reactions of $Fe(CO)_3$.[25] The reaction of $Fe(CO)_3 + Fe(CO)_5$ to form the bridged form of $Fe_2(CO)_8$ is facile, suggesting that the ground state of this form of $Fe_2(CO)_8$ is a triplet.[25] Formation of the unbridged form of $Fe_2(CO)_8$ from these same reactants is currently under study.[25] Spin conservation rules suggest that the $Ru(CO)_3$ and $Ru(CO)_4$ fragments are likely to possess ground-state electronic singlet configurations on the basis of the magnitude of their reaction rate constants. A singlet ground-state configuration for $Ru(CO)_4$ has been predicted as lowest in energy based on Hartree–Fock–Slater molecular orbital calculations.[31] Low-spin configurations are most often observed for second- and third-row transition-metal complexes. For third-row transition elements, it has been noted that spin-selection rules can break down from effects such as large spin–orbit coupling.[32] Indeed, this trend is evident in the atomic electronic spectra of the transition elements.[33] For example, very few of the most intense spectral lines for first-row metals arise from spin-forbidden transitions, whereas for third-row elements, transitions that give intense spectral features do not show a significant bias toward following spin-selectron rules. The assumption that the $Os(CO)_3$ and $OsCO)_4$ species possess ground-state singlet electronic states cannot be concluded solely on the basis of evidence from rate constants. However, our observations are compatible with that assignment.

(30) Seder, T. A.; Ouderkirk, A. J.; Weitz, E. *J. Chem. Phys.* **1986**, *85*, 1977.
(31) Ziegler, T. *Inorg. Chem.* **1986**, *25*, 2721.
(32) Steinfeld, J. I. *Molecules and Radiation*; Harper and Row: New York, 1974.
(33) Meggers, W. F; Corliss, C. H.; Scribner, B. F. *Tables of Spectral Line Intensities*; NBS Monograph 32; National Bureau of Standards: Washington, 1961.

Conclusions

The transient infrared spectroscopy study of unsaturated osmium carbonyl complexes generated by 248-nm photolysis of $Os(CO)_5$ has shown that $Os(CO)_3$ and $Os(CO)_4$ species are the nascent photoproducts. With 248-nm irradiation, the predominant photoproduct of $M(CO)_5$ is $Fe(CO)_2$ for iron and $M(CO)_3$ for ruthenium and osmium. The average metal carbonyl bond dissociation energy for loss of three CO ligands is larger for ruthenium and osmium than for iron. Two dinuclear osmium carbonyl complexes, $Os_2(CO)_8$ and $Os_2(CO)_9$, are formed by reactions of the unsaturated photofragments with parent $Os(CO)_5$; $Os_2(CO)_8$ had not been reported previously. There is evidence for formation of trinuclear osmium clusters from reaction of $Os_2(CO)_8$ with $Os(CO)_5$. The tendency for cluster formation for osmium is reflected in the additional depletion of $Os(CO)_5$ between UV pulses that is several times the amount photolyzed. The bimolecular rate constants for reaction of $Os(CO)_3$ and $Os(CO)_4$ with CO are 7.6 ± 0.9 and $5.5 \pm 0.6 \times 10^{-11}$ cm^3 molecule^{-1} s^{-1}, respectively. These are the same magnitude as those observed for the corresponding ruthenium complexes and 10^3 larger than that observed for the reaction of $Fe(CO)_4$ with CO. The rate constant for formation of $Os_2(CO)_8$ is $2.7 \pm 0.9 \times 10^{-10}$ cm^3 molecule^{-1} s^{-1} and is similar to that for $Fe_2(CO)_8$. All photofragments for the group 8 pentacarbonyls have very short gas phase lifetimes except for $Fe(CO)_4$. Slow reaction rates for $Fe(CO)_4$ are explained on the basis of spin selection rules. Ruthenium carbonyl photofragments are thought to have singlet electronic ground states. The behavior of $Os(CO)_x$ photofragments is consistent with spin conservation during reactions with CO or parent. However, due to enhanced spin–orbit coupling in heavy metals, spin states are expected to have significantly less effect on reaction rate for osmium species than for iron or even ruthenium. Thus it is premature to conclude that the ground states of $Os(CO)_x$ fragments *must* be singlets based on this kinetic evidence, though their behavior is compatible with this conclusion.

Acknowledgment. We are indebted to G.-Y. Kiel and Prof. J. Takats for providing the $Os(CO)_5$ for this study. We thank the National Science Foundation for support of this work under NSF Grant CHE 88-06020 and we acknowledge support of the donors of the Petroleum Research Fund, administered by the American Chemical Society.

Excited-State Calorimetry Studies of Triplet Benzophenone Using Time-Resolved Photothermal Beam Deflection Spectroscopy

P. E. Poston and J. M. Harris*

Contribution from the Department of Chemistry, University of Utah, Salt Lake City, Utah 84112. *Received June 21, 1989*

Abstract: Photothermal beam deflection spectroscopy is found to be a useful method for determining the kinetics and energetics of photochemical and photophysical processes. The accumulation of heat from the reaction and decay of excited states is observed with a step-response function on time scales from nanoseconds to milliseconds. Using this method, we study hydrogen abstraction from ethanol by triplet benzophenone and determine the rate constant of this reaction to be 1.43 (±0.08) × 10^6 M^{-1} s^{-1}. From the relative amplitudes of the photothermal transients, we derive the enthalpy of the photoproducts and estimate the C–H bond dissociation energy of benzhydrol and the O–H bond energy of the ketyl radical to be 87 (±2) and 95 (±2) kcal/mol, respectively. We also investigate the intensity dependence of heat released from triplet benzophenone to determine the influence of excited-state absorption on the calorimetric results. The data are fit to a four-level, excited-state absorption model, and the triplet excited-state absorption cross section of benzophenone at 322 nm is found to be 2.7 (±0.5) × 10^{-17} cm^2.

Photothermal spectroscopy with pulsed-laser sources is developing into a powerful method for determining nonradiative, excited-state quantum yields and decay kinetics of molecules in solution. The measurement is a specific example of photocalorimetry where the heat given off by the decay of excited states and/or photoproducts is observed as an increase in the sample temperature. Early photocalorimetry experiments produced excited states with a continuous source and detected the temperature

0002-7863/90/1512-644$02.50/0